

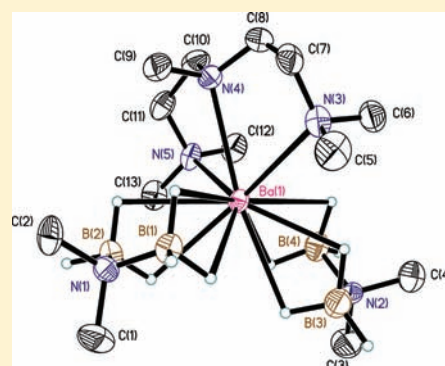
Synthesis and Structural Diversity of Barium (*N,N*-Dimethylamino)diboranates

Scott R. Daly, Brian J. Bellott, Mark A. Nesbit, and Gregory S. Girolami*

The School of Chemical Sciences, University of Illinois at Urbana–Champaign, 600 South Mathews Avenue, Urbana, Illinois 61801, United States

Supporting Information

ABSTRACT: The reaction of a slurry of BaBr₂ in a minimal amount of tetrahydrofuran (THF) with 2 equiv of Na(H₃BNMe₂BH₃) in diethyl ether followed by crystallization from diethyl ether at –20 °C yields crystals of Ba(H₃BNMe₂BH₃)₂(Et₂O)₂ (**1**). Drying **1** at room temperature under vacuum gives the partially desolvated analogue Ba(H₃BNMe₂BH₃)₂(Et₂O)_x (**1'**) as a free-flowing white solid, where the value of *x* varies from <0.1 to about 0.4 depending on whether desolvation is carried out with or without heating. The reaction of **1** or **1'** with Lewis bases that bind more strongly to barium than diethyl ether results in the formation of new complexes Ba(H₃BNMe₂BH₃)₂(L), where L = 1,2-dimethoxyethane (**2**), *N,N,N',N'*-tetramethylethylenediamine (**3**), 12-crown-4 (**4**), 18-crown-6 (**5**), *N,N,N',N'*-tetraethylethylenediamine (**6**), and *N,N,N',N',N''*-pentamethylethylenetriamine (**7**). Recrystallization of **4** and **5** from THF affords the related compounds Ba(H₃BNMe₂BH₃)₂(12-crown-4)(THF)·THF (**4'**) and Ba(H₃BNMe₂BH₃)₂(18-crown-6)·2THF (**5'**). In addition, the reaction of BaBr₂ with 2 equiv of Na(H₃BNMe₂BH₃) in the presence of diglyme yields Ba(H₃BNMe₂BH₃)₂(diglyme)₂ (**8**), and the reaction of **1** with 15-crown-5 affords the diadduct [Ba(15-crown-5)₂][H₃BNMe₂BH₃]₂ (**9**). Finally, the reaction of BaBr₂ with Na(H₃BNMe₂BH₃) in THF, followed by the addition of 12-crown-4, affords the unusual salt [Na(12-crown-4)₂][Ba(H₃BNMe₂BH₃)₃(THF)₂] (**10**). All of these complexes have been characterized by IR and ¹H and ¹¹B NMR spectroscopy, and the structures of compounds **1–3**, **4'**, **5'**, and **6–10** have been determined by single-crystal X-ray diffraction. As the steric demand of the Lewis bases increases, the structure changes from polymers to dimers to monomers and then to charge-separated species. Despite the fact that several of the barium complexes are monomeric in the solid state, none is appreciably volatile up to 200 °C at 10^{–2} Torr.



INTRODUCTION

Barium is a constituent in a wide variety of materials that have properties useful for electronic applications. For example, the versatile and ubiquitous BaTiO₃, a ferroelectric ceramic, has been extensively used in electronic devices because it has a high dielectric constant as well as piezoelectric and thermoresistive properties.^{1–4} The cuprate YBa₂Cu₃O_{7–x} and similar derivatives are high-*T_c* superconductors and were the first materials to be superconducting above the boiling point of nitrogen.^{5–9} Another example of the utility of barium-containing materials is the use of the optoelectronic material β-BaB₂O₄ in nonlinear optical devices and solid-state UV lasers.^{10,11}

Chemical vapor deposition (CVD) and atomic layer deposition are useful methods for depositing thin films on substrates with advanced architectures and high aspect ratios, such as those found in the majority of electronic devices.^{12,13} One limitation, however, to preparing barium-containing materials by these methods is the scarcity of barium precursors with adequate volatility.^{14,15} Although volatile barium complexes are known, few such compounds have vapor pressures high enough to grow conformal films by CVD.^{12,16} Molecular barium complexes often suffer from low volatility because the large radius of Ba²⁺ makes it difficult to prepare electrically neutral complexes that

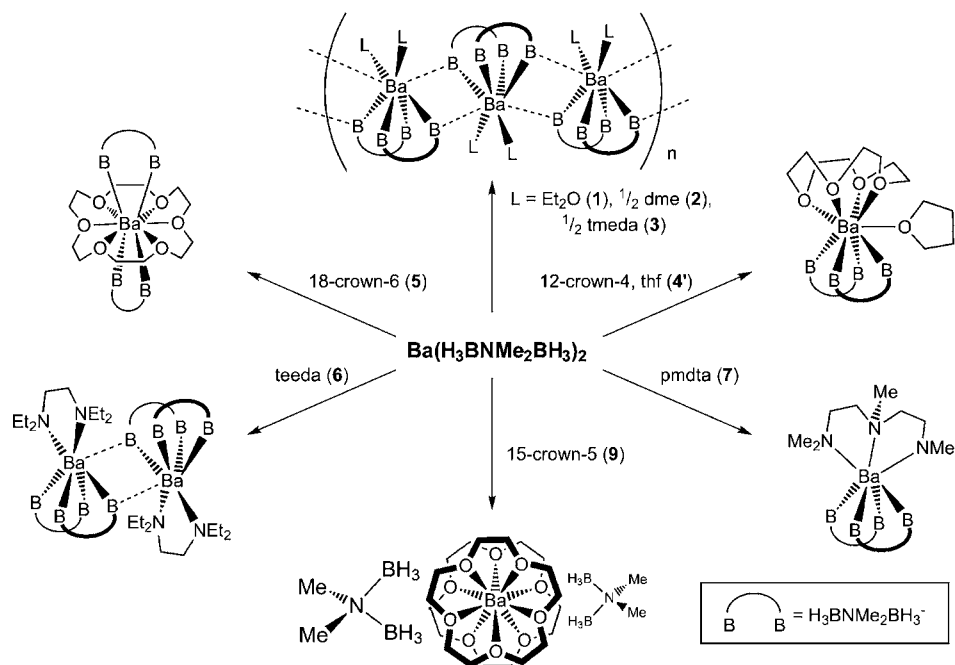
are both monomeric and free of weakly bound ligands that dissociate upon heating.^{17–22} One successful strategy to obtain volatile barium complexes is to employ multidentate ligands that can encapsulate the metal.¹⁵ For example, neutral ancillary ligands, such as glymes, can be used to help fill the coordination sphere if the anionic ligands themselves are not sufficiently saturating.²³ The majority of barium complexes that have been explored as thin-film precursors are diketonates or ketoimines,^{24–34} and often these ligands have been functionalized with flexible donor pendants that can occupy additional coordination sites around the metal.^{22,35–38} Other barium precursors that have been used for thin-film growth include those that utilize alkoxide³⁹ cyclopentadienyl,^{40–45} and (pyrazolyl)borate ligands.^{46–48}

Some transition-metal borohydride (BH₄[–]) complexes are highly volatile and have proven to be outstanding CVD precursors for the deposition of metal diboride films.^{49–56} Despite these successes, alkaline-earth tetrahydroborate complexes are often polymeric and few if any meet the volatility requirements for CVD, which can be attributed to the small size of BH₄[–] in

Received: August 3, 2011

Published: June 5, 2012

Scheme 1



relation to these large metal ions.^{57,58} We have recently shown, however, that the larger chelating borohydrides octahydrotriborate, $[\text{B}_3\text{H}_8]^-$,⁵⁹ and (*N,N*-dimethylamino)diboranate, $[\text{H}_3\text{BNMe}_2\text{BH}_3]^-$,^{60–62} can be used to prepare highly volatile magnesium complexes.^{63,64} These sterically larger borohydride ligands are able to saturate more of the magnesium coordination sphere, thereby inhibiting polymeric bonding modes and yielding highly volatile complexes such as $\text{Mg}(\text{H}_3\text{BNMe}_2\text{BH}_3)_2$.⁶⁴ Some of these complexes are outstanding CVD precursors: in a particularly dramatic example, $\text{Mg}(\text{H}_3\text{BNMe}_2\text{BH}_3)_2$ has been used to grow superconformal MgO films by CVD using water as a secondary reactant.⁶⁵ Prompted by importance of barium in electronic materials and the potential of $[\text{H}_3\text{BNMe}_2\text{BH}_3]^-$ to produce viable CVD precursors,^{65,66} we now describe the preparation and characterization of a series of new barium (*N,N*-dimethylamino)diboranate complexes.

RESULTS

Synthesis of Barium (*N,N*-Dimethylamino)diboranates. The treatment of a slurry of BaBr_2 in a minimal amount of tetrahydrofuran (THF) with 2 equiv of $\text{Na}(\text{H}_3\text{BNMe}_2\text{BH}_3)$ in diethyl ether, followed by removal of the solvent and crystallization from diethyl ether at -20°C , yields crystals of $\text{Ba}(\text{H}_3\text{BNMe}_2\text{BH}_3)_2(\text{Et}_2\text{O})_2$ (**1**). The reaction does not occur in the absence of THF despite the fact that $\text{Na}(\text{H}_3\text{BNMe}_2\text{BH}_3)$ is readily soluble in Et_2O , suggesting that some dissolution of BaBr_2 is also required for the reaction to proceed. Drying **1** under vacuum gives the desolvated analogue $\text{Ba}(\text{H}_3\text{BNMe}_2\text{BH}_3)_2(\text{Et}_2\text{O})_x$ (**1'**), as a free-flowing white solid, where the value of *x* varies from <0.1 to about 0.4 depending on whether the compound is heated during desolvation.

Neither **1** nor **1'** is volatile, in part because they have polymeric structures (see below). Accordingly, we investigated the synthesis of analogues of **1** with more strongly coordinating Lewis bases that might form monomeric complexes capable of being sublimed in vacuum. We find that the treatment of **1** or **1'** with 1,2-dimethoxyethane (DME), *N,N,N',N'*-tetramethylethylenediamine

(TMEDA), or 1,4,7,10-tetraoxacyclododecane (12-crown-4) in diethyl ether results in the formation of new complexes $\text{Ba}(\text{H}_3\text{BNMe}_2\text{BH}_3)_2(\text{DME})$ (**2**), $\text{Ba}(\text{H}_3\text{BNMe}_2\text{BH}_3)_2(\text{TMEDA})$ (**3**), and $\text{Ba}(\text{H}_3\text{BNMe}_2\text{BH}_3)_2(12\text{-crown-4})$ (**4**) (Scheme 1). Additionally, we find that the treatment of **1'** with 1,4,7,10,13,16-hexaoxacyclohexadecane (18-crown-6), *N,N,N',N'*-tetraethylethylenediamine (TEEDA), or *N,N,N',N',N'*-pentamethylethylenetriamine (PMDTA) in THF yields the new complexes $\text{Ba}(\text{H}_3\text{BNMe}_2\text{BH}_3)_2(18\text{-crown-6})$ (**5**), $\text{Ba}(\text{H}_3\text{BNMe}_2\text{BH}_3)_2(\text{TEEDA})$ (**6**), and $\text{Ba}(\text{H}_3\text{BNMe}_2\text{BH}_3)_2(\text{PMDTA})$ (**7**), respectively. Adducts of this type can also be made directly from BaBr_2 ; thus, the reaction of BaBr_2 with 2 equiv of $\text{Na}(\text{H}_3\text{BNMe}_2\text{BH}_3)$ in bis(2-methoxyethyl) ether (diglyme) yields $\text{Ba}(\text{H}_3\text{BNMe}_2\text{BH}_3)_2(\text{diglyme})_2$ (**8**). Interestingly, the treatment of **1'** with 1,4,7,10,13-pentaoxacyclopentadecane (15-crown-5) affords the diadduct $[\text{Ba}(15\text{-crown-5})_2][\text{H}_3\text{BNMe}_2\text{BH}_3]_2$ (**9**), even if only 1 equiv of 15-crown-5 is added per barium.

Complexes **2–9** retain their coordinated bases even when exposed to a dynamic vacuum over extended periods at room temperature. Recrystallization of **4** and **5** from THF affords the related compounds $\text{Ba}(\text{H}_3\text{BNMe}_2\text{BH}_3)_2(12\text{-crown-4})(\text{THF})\cdot\text{THF}$ (**4'**) and $\text{Ba}(\text{H}_3\text{BNMe}_2\text{BH}_3)_2(18\text{-crown-6})\cdot 2\text{THF}$ (**5'**). Finally, the reaction of BaBr_2 with $\text{Na}(\text{H}_3\text{BNMe}_2\text{BH}_3)$ in THF, followed by the addition of 12-crown-4, gives a clear solution from which the unusual salt $[\text{Na}(12\text{-crown-4})_2][\text{Ba}(\text{H}_3\text{BNMe}_2\text{BH}_3)_3(\text{THF})_2]$ (**10**) can be isolated.

Molecular Structures. The molecular structures of the new barium complexes **1–3**, **4'**, **5'**, and **6–10** were determined by single-crystal X-ray diffraction. In the following discussions of the structures, we will adopt two strategies. First, we will describe the coordination polyhedron as if each BH_3 group interacting with the barium center occupies one coordination site. Second, we will give the actual coordination number, in which each B–H–M bridging unit occupies one coordination site. In general, we will not attempt to describe the coordination polyhedron that corresponds with this second view, in part because the exact locations of the hydrogen atoms are subject to some uncertainty but also because describing polyhedra

with 11 or more vertices is often problematic, especially if the symmetry is low.

In the Et₂O adduct **1**, each barium atom resides on a 2-fold axis and is coordinated to two chelating [H₃BNMe₂BH₃][−] (DMADB) ligands and to two diethyl ether molecules. In addition, each barium center is coordinated to two BH₃ groups from DMADB ligands on adjacent barium centers. Owing to the latter bridging interactions, the Ba(H₃BNMe₂BH₃)₂(Et₂O)₂ units are linked into a polymeric chain (Figure 1). The boron

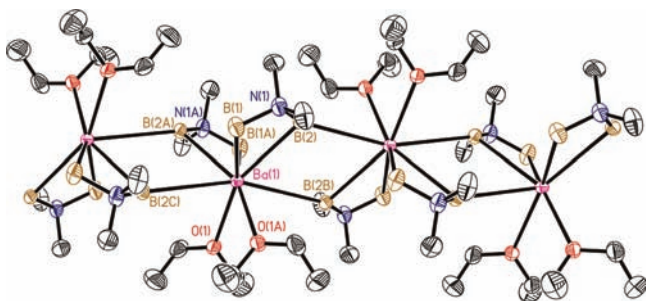


Figure 1. Portion of the polymeric structure of **1**. Ellipsoids are drawn at the 35% probability level. The hydrogen atoms have been removed for clarity; see the Supporting Information for a view of the structure with hydrogen atoms on boron included.

and oxygen atoms describe a distorted bicapped trigonal prism around each barium center, in which the two bridging boron atoms cap two of the square faces. Boron atoms B(1), B(2), and O(1A) define one of the distorted triangular faces of the inner trigonal prism, and their 2-fold related counterparts B(1A), B(2A), and O(1) define the other.

The Ba⋯B distances to the chelating DMADB ligands in **1** are 3.216(6) and 3.265(6) Å; in contrast, the Ba⋯B distances to the BH₃ groups from neighboring centers in the chain are much longer at 3.477(5) Å (Tables 1 and 2). The location of the hydrogen atoms provides an explanation of this difference. The shorter Ba⋯B contacts (to the BH₃ groups of the chelating DMADB ligands) are each κ^2H interactions, whereas the longer Ba⋯B contacts (to the BH₃ groups of DMADB ligands that

chelate to neighboring barium centers) are κ^1H interactions. The two BH₃ groups within each DMADB ligand are different: one of the BH₃ groups interacts with only one barium center, whereas the other interacts with two. In all, the barium centers in **1** are 12-coordinate and are bound to 10 hydrogen atoms and 2 oxygen atoms.

The Ba⋯B distances are consistent with those seen in other barium borohydride complexes. For example, in Ba(BH₃R)₂(L)_x complexes (where R = H or PMe₂[C(SiMe₃)₂] and L = THF, diglyme, or 18-crown-6), the Ba⋯B distances to the bound κ^3H -BH₃R groups range from 2.975(9) to 3.063(6) Å.^{57,67} These comparisons show that the Ba⋯B distance decreases by ~0.2 Å as the denticity of the borohydride group increases by one (i.e., from κ^1H to κ^2H or from κ^2H to κ^3H). The Ba–O distances in the Ba(BH₃R)₂(L)_x complexes, which range from 2.707(3) to 2.895(4) Å, compare well with those of 2.800(3) Å for the coordinated diethyl ether molecules in **1**.

The structure of the DME adduct **2** is also polymeric, and the coordination geometry is very similar to that of **1** (Figure S1 in the Supporting Information). The two oxygen atoms of the coordinated DME molecule occupy the same coordination sites that the two Et₂O molecules occupy in **1**. The chelating and bridging Ba⋯B distances of 3.251(3)–3.271(3) and 3.412(3)–3.461(3) Å, respectively, are similar to those in **1**, as are the Ba–O distances of 2.815(2) and 2.823(2) Å (Table 1).

The structure of the TMEDA adduct **3** is also similar except that the bridging Ba⋯B distance of 3.512(3) Å is ~0.05 Å longer than those in **1** and **2**, which can be attributed to the increased steric bulk of the TMEDA ligand relative to Et₂O and DME (Figure S2 in the Supporting Information). As seen in **1** and **2**, the Ba⋯B(2) distance of 3.261(3) Å to the κ^2H BH₃ groups that are both chelating and bridging to an adjacent metal is ~0.02 Å (i.e., negligibly) longer than the Ba⋯B(1) distance of 3.237(3) Å to the κ^2H BH₃ groups that have no bridging interaction (Table 1). The Ba–N distance to the coordinated TMEDA molecule of 2.996(2) Å is ca. 0.2 Å longer than the Ba–O distances observed in **1** and **2**. This difference, which is chemically significant and much larger than the 0.03 Å difference in atomic radii between oxygen and nitrogen atoms,

Table 1. Selected Bond Distances (Å) for Barium (*N,N*-Dimethylamino)diboranates

	1 (L = Et ₂ O)	2 (L = DME)	3 (L = TMEDA)	4' (L = 12-crown-4)	5' (L = 18-crown-6)	6 (L = TEEDA)	7 (L = PMDTA)	8 (L = diglyme)	9 (L = 15-crown-5)	10 (Na salt)
Ba⋯B	3.216(6) 3.265(6)	3.251(3) 3.252(3) 3.260(3) 3.271(2)	3.237(3) 3.261(3)	3.270(7) 3.399(7) 3.278(7) 3.316(8)	3.354(16) 3.396(13) 3.458(14) 3.458(15)	3.243(4) 3.255(5) 3.191(6) 3.173(6)	3.158(7) 3.173(7) 3.262(9) 3.163(8)	3.266(3) 3.280(3) 3.051(2)		3.255(5) 3.258(6) 3.260(5) 3.237(5) 3.255(6) 3.291(6)
Ba⋯B'	3.477(5)	3.412(3) 3.461(3)	3.512(3)			3.324(5)				
Ba–O	2.800(3)	2.815(1) 2.823(1)		2.854(4) ^a 2.864(4) 2.904(4) 2.922(4) 2.838(4)	2.789(3) 2.792(3) 2.798(3)		2.947(1) 2.835(1) 2.970(1) 2.890(1) 2.954(1) 2.827(1)	2.813(3) 2.815(3) 2.824(3) 2.891(3) 2.818(3)	2.871(3) 2.867(3)	
Ba–N			2.996(1)			2.970(0) 2.947(4)	2.905(5) 2.916(4) 2.884(4)			

^aBa–O bond to coordinated THF.

Table 2. Crystallographic Data for the Barium (N,N-Dimethylamino)diboranate Complexes at 193(2) K

	1 (L = Et ₂ O)	2 (L = DME)	3 (L = TMEDA)	4' (L = 12-crown-4)	5' (L = 18-crown-6)	6 (L = TEEDA)	7 (L = PMDTA)	8 (L = diglyme)	9 (L = 15-crown-5)	10 (Na salt)
formula	C ₁₂ H ₁₄ B ₄ N ₂ O ₂ Ba	C ₈ H ₈ B ₄ N ₂ O ₂ Ba	C ₁₀ H ₁₀ B ₄ N ₂ Ba	C ₁₀ H ₁₂ N ₂ O ₂ B ₄ Ba	C ₂₄ H ₂₈ B ₄ N ₂ O ₈	C ₂₈ H ₃₆ B ₈ N ₈ Ba ₂	C ₁₃ H ₁₇ B ₄ N ₂ Ba	C ₂₀ H ₃₂ B ₄ N ₂ O ₂ Ba	C ₂₄ H ₄₀ B ₄ Ba ₂ N ₂ O ₁₀	C ₃₀ H ₃₆ B ₆ N ₂ O ₁₀ NaBa
fw (g mol ⁻¹)	429.07	370.77	397.04	549.18	689.35	906.26	454.12	597.22	721.35	872.19
λ (Å)	0.71073	0.71073	0.71073	0.71073	0.71073	0.71073	0.71073	0.71073	0.71073	0.71073
cryst syst	monoclinic	monoclinic	monoclinic	monoclinic	orthorhombic	triclinic	monoclinic	triclinic	monoclinic	triclinic
space group	C ₂ /c	P2 ₁ /c	C ₂ /c	P2 ₁ /c	Pnma	P1	P2 ₁ /n	P1	P2 ₁ /c	P1
a (Å)	21.8381(12)	10.384(3)	21.1428(5)	9.147(3)	10.1886(8)	9.555(3)	9.544(3)	11.8304(4)	9.6288(6)	12.7000(7)
b (Å)	11.0420(6)	17.411(5)	10.3259(2)	17.141(5)	24.5226(17)	12.341(4)	18.799(6)	16.8151(6)	10.7092(7)	21.3688(11)
c (Å)	10.7710(6)	10.679(3)	10.6711(2)	18.377(5)	14.6894(10)	12.448(4)	14.610(5)	16.8646(6)	17.7185(13)	21.5299(11)
α (deg)	90	90	90	90	90	64.618(4)	90	71.134(2)	90	60.409(2)
β (deg)	117.704(3)	104.108(4)	116.4000(10)	90.453(4)	90	81.444(5)	95.937(6)	83.495(2)	92.031	89.888(3)
γ (deg)	90	90	90	90	90	71.243(5)	90	87.735(2)	90	72.825(3)
V (Å ³)	2299.5(2)	1872.6(9)	2086.74(7)	2881.3(14)	3670.2(5)	1255.6(7)	2607.2(14)	3154.18(19)	1825.9(2)	4780.9(4)
Z	4	4	4	4	4	1	4	4	2	4
ρ _{calc} (g cm ⁻³)	1.239	1.316	1.264	1.266	1.248	1.199	1.157	1.258	1.132	1.212
μ (mm ⁻¹)	1.730	2.113	1.897	1.406	1.122	1.584	1.527	1.29	1.134	0.886
R(int)	0.0683	0.0390	0.0519	0.0559	0.2185	0.1386	0.0477	0.0979	0.1960	0.1408
abs corr	face-indexed	face-indexed	face-indexed	face-indexed	face-indexed	face-indexed	face-indexed	face-indexed	face-indexed	face-indexed
method										
max/min transmn factors	0.883/0.483	0.817/0.476	0.964/0.654	0.819/0.506	0.912/0.706	0.767/0.542	0.532/0.593	0.946/0.841	0.895/0.563	0.652/0.884
data/restraints/params	2112/0/124	3414/0/290	2157/0/167	7049/13/319	4150/8/238	4783/0/254	4479/34/253	11 617/298/758	4043/106/246	21 327/2079/1403
GOF on F ²	1.031	0.891	0.880	0.847	1.051	0.990	0.751	0.789	1.023	0.901
R1 [I > 2σ(I)] ^a	0.0325	0.0155	0.0206	0.0228	0.0461	0.0376	0.0369	0.0433	0.0458	0.0468
wR2 (all data) ^b	0.0792	0.0304	0.0307	0.0442	0.1465	0.0805	0.0782	0.0751	0.1344	0.1123
max, min Δρ _{electron} (e Å ⁻³)	1.035/-0.531	0.800/-0.330	0.395/-0.338	1.616/-0.766	0.795/-0.973	2.214/-0.929	0.901/-0.713	0.895/-0.496	1.604/-1.189	2.188/-1.271

^aR1 = $\sum |F_o| - |F_c| / \sum |F_o|$ for reflections with $F_o^2 > 2\sigma(F_o^2)$. ^bwR2 = $[\sum w(F_o^2 - F_c^2)^2 / \sum (F_o^2)^2]^{1/2}$ for all reflections.

most likely reflects the larger degree of steric crowding in **3** and the consequent lengthening of the Ba–N bond relative to Ba–O.⁶⁸

X-ray-quality crystals of the 12-crown-4 adduct **4** could not be grown, but cooling concentrated solutions of **4** in THF yielded **4'**, which has the stoichiometry Ba(H₃BNMe₂BH₃)₂(12-crown-4)(THF) and differs from **4** in that a molecule of THF has been added to the coordination sphere of the barium atom. Unlike the polymeric structures of **1–3**, compound **4'** is a monomer. If each BH₃ group is considered to occupy one coordination site, then the coordination geometry of the barium center in **4'** is best described as a distorted capped square prism, in which the THF molecule caps the square face formed by atoms B(1), B(3), O(13), and O(14) (Figure 2). Boron

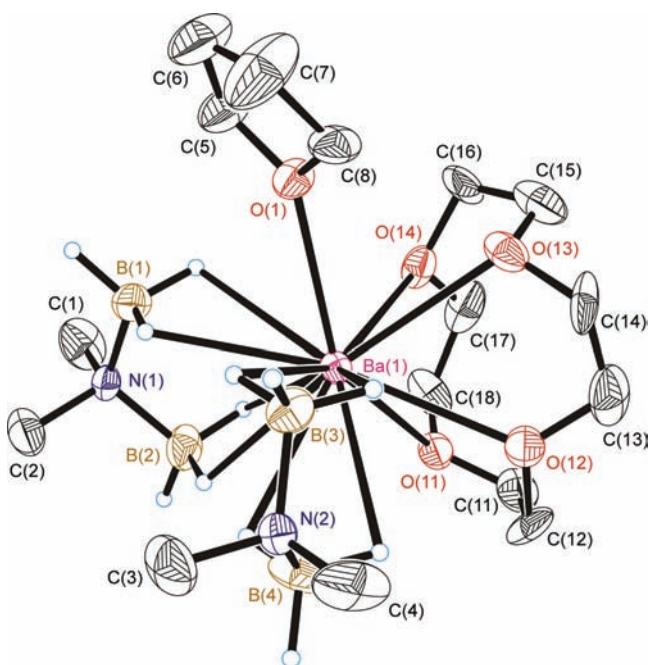


Figure 2. Molecular structure of **4'**. Ellipsoids are drawn at the 35% probability level. The hydrogen atoms attached to carbon atoms have been removed for clarity.

atoms B(2) and B(4), which are located closest to the 12-crown-4 molecule, form Ba···B distances of 3.399(7) and 3.316(8) Å that are longer than the Ba(1)···B(1) and Ba(1)···B(3) distances, which are 3.270(7) and 3.278(7) Å (Table 1). All of these entail κ^2H interactions, so that the overall coordination number of the barium center is 13 (eight hydrogen atoms and five oxygen atoms). The Ba–O distances to the THF and 12-crown-4 ligands range from 2.838(4)–2.922(4) Å and are longer than those in **1** and **2**, which may be attributed to the higher coordination number of 13 in compound **4'** versus 12 in **1** and **2**.

X-ray-quality crystals of the 18-crown-6 adduct **5'** were grown from THF; **5'** differs from **5** in that it contains two molecules of THF per formula unit, but these molecules are not bound to the barium centers. If each BH₃ group is considered to occupy one coordination site, then the coordination environment about the barium center can be described as a hexagonal bipyramid in which the two axial vertices of the bipyramid are bifurcated; in this view, the four boron atoms are the bifurcated vertices and the six oxygen atoms in the 18-crown-6 ring describe the base of the pyramids (Figure 3). The Ba···B distances, which range from 3.354(16) to 3.458(15) Å, are

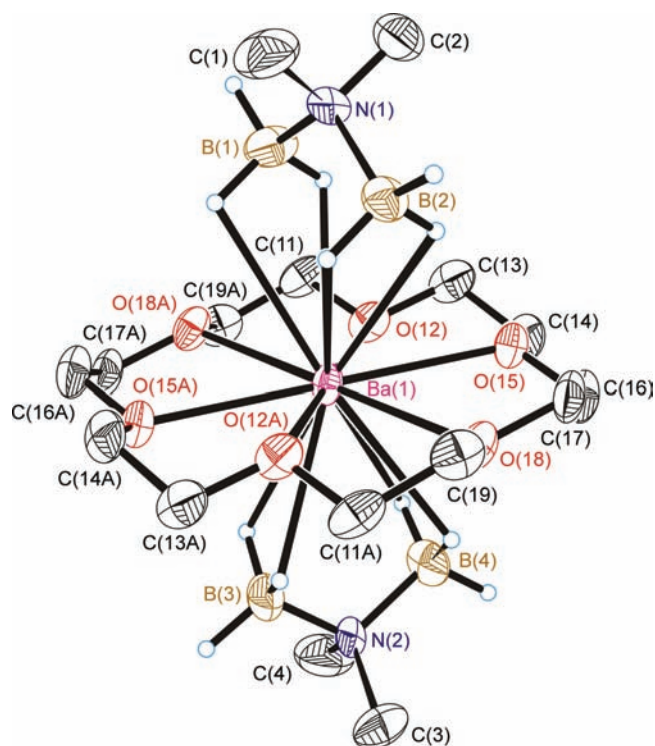


Figure 3. Molecular structure of **5'**. Ellipsoids are drawn at the 35% probability level. The THF molecules of solvation and the hydrogen atoms attached to carbon atoms have been removed for clarity.

significantly longer than those observed for any of the other barium complexes in this paper. The long Ba···B distances in **5'** are evidence of a high degree of steric crowding. Indeed, the coordination number of 14 (eight hydrogen atoms and six oxygen atoms) is the largest of the complexes that we have made.

X-ray-quality crystals of the TEEDA compound **6** reveal that each barium atom is bound to two κ^2H -H₃BNMe₂BH₃- κ^2H ligands and one chelating TEEDA ligand (Figure 4). Each barium center also forms a bond to a hydrogen atom on one of the chelating aminodiborane ligands on a neighboring barium center, similar to the bridging interactions observed for **1–3**. The intermolecular bonding does not propagate beyond a dimer, however, because of the steric effects of the ethyl groups on TEEDA (compared to the smaller methyl groups on TMEDA in **3**). If each BH₃ unit is considered to occupy one coordination site (and the one bridging hydrogen atom is ignored), then the structure can be thought of as a capped trigonal prism in which B(1A) caps the face formed by B(3), B(1), and B(2). Overall, the barium centers are 11-coordinate (nine hydrogen atoms and two nitrogen atoms).

The PMDTA complex (**7**) is a monomer in which both aminodiborane ligands coordinate in a κ^2H -H₃BNMe₂BH₃- κ^2H fashion, and the PMDTA ligand binds by means of all three of its nitrogen atoms (Figure 5). If each BH₃ group is considered to occupy one coordination site, then the geometry about the barium center can be considered as a distorted square-capped trigonal prism in which B(3) caps the face formed by B(1), B(2), B(4), and N(3). Consistent with this view, the Ba(1)···B(1), Ba(1)···B(2), and Ba(1)···B(4) distances are 3.158(7)–3.173(7) Å, but the Ba(1)···B(3) distance of 3.262(9) Å is distinctly longer. The Ba–N distances to the PMDTA ligand are 2.884(4)–2.916(4) Å. Overall, the

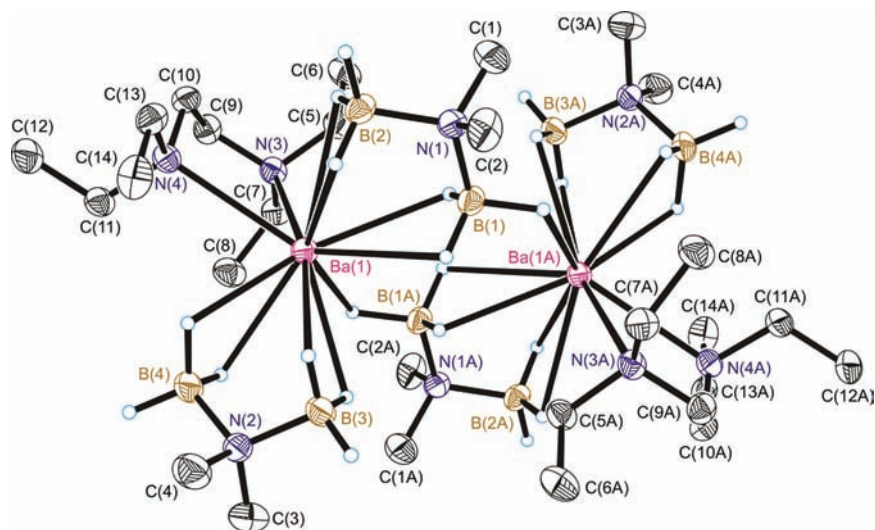


Figure 4. Molecular structure of **6**. Ellipsoids are drawn at the 35% probability level. The hydrogen atoms attached to carbon atoms have been omitted for clarity.

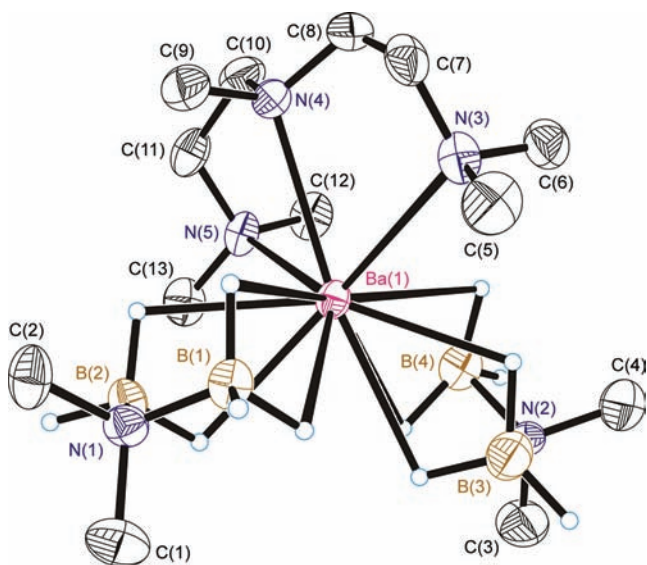


Figure 5. Molecular structure of **7**. Ellipsoids are drawn at the 35% probability level, except for hydrogen atoms, which are represented by arbitrarily sized spheres.

barium atom is 11-coordinate, with eight hydrogen atoms and three nitrogen atoms defining the inner coordination sphere.

For the bis(diglyme) adduct, **8**, one of the DMADB ligands chelates to the barium center in a typical κ^2H - $H_3BNMe_2BH_3$ - κ^2H fashion, but the other DMADB ligand binds to the metal by means of only one BH_3 group in a κ^3H fashion (Figure 6). The two DMADB ligands are arranged trans with respect to one another; the two diglyme molecules are approximately coplanar and form an equatorial belt. The six equatorial oxygen atoms and the three barium-bound boron atoms describe a nine-coordinate polyhedron that has been given the plebeian name of “the hula hoop”.⁶⁹ The idealized hula hoop polyhedron, which has C_{2v} symmetry, consists of a planar hexagonal girdle capped on one side by a single vertex and on the other side by a pair of vertices. In **9**, the six oxygen atoms of the two diglyme molecules are not exactly coplanar and deviate more or less from the mean plane in order to accommodate the steric demands of the chelating DMADB ligand. As a result, the

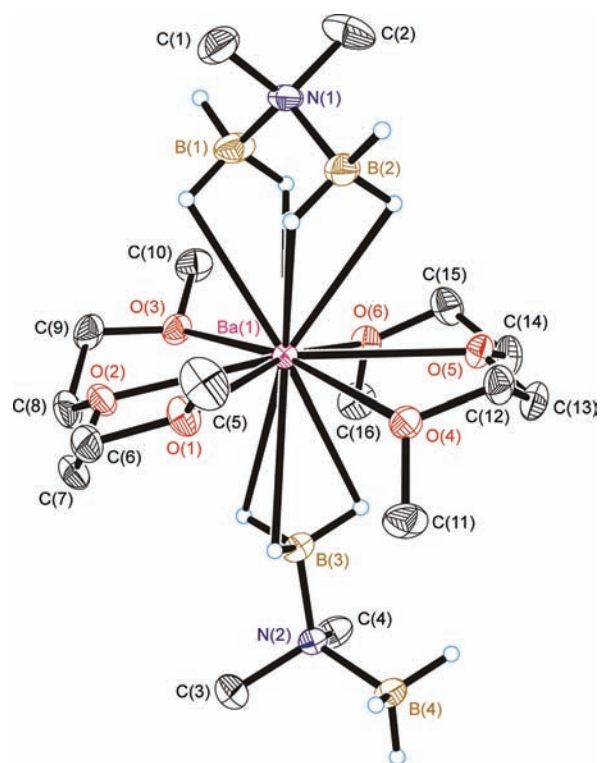


Figure 6. Molecular structure of **8**. Ellipsoids are drawn at the 35% probability level. The hydrogen atoms attached to carbon atoms have been removed for clarity.

B – Ba – O angles to the κ^3H -DMADB ligand of $79.58(5)$ – $88.74(5)^\circ$ are all less than the ideal 90° angle (Table S8 in the Supporting Information). A few other complexes have been described that adopt a hula hoop geometry; the present complex, however, is evidently the first to adopt it without the constraints of a cyclic hexadentate ligand. Overall, the barium atom forms bonds with seven hydrogen atoms and six oxygen atoms, so that the total coordination number is 13.

The $Ba\cdots B$ distances of $3.266(3)$ and $3.280(3)$ Å to the chelating DMADB ligand in **8** are similar to those seen in **1**–**4**. In contrast, the $Ba\cdots B$ distance of $3.051(2)$ Å to the κ^3H -DMADB

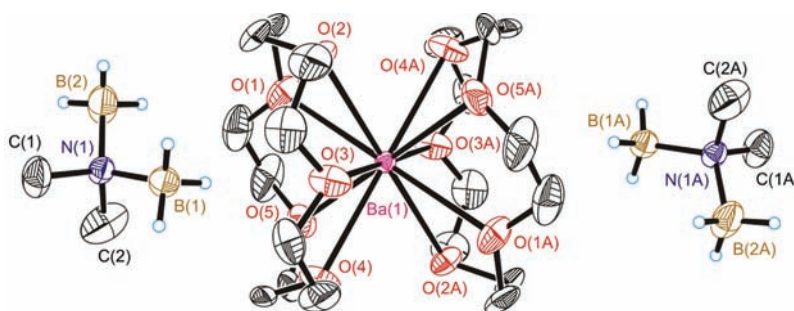


Figure 7. Molecular structure of **9**. Ellipsoids are drawn at the 35% probability level. The hydrogen atoms attached to carbon atoms have been removed for clarity.

ligand in **8** is much shorter, as expected from the increased denticity. This Ba...B distance is similar to those reported for the $\text{Ba}(\text{BH}_3\text{R})_2(\text{L})_x$ complexes mentioned above, which also contain metal-bound $\kappa^3\text{H-BH}_3\text{R}$ groups.^{57,67} The Ba–O bond distances, which range from 2.827(1) to 2.970(1) Å, are longer than those observed for **1**, **2**, and **4'**, probably owing to the increased crowding around the metal because of the arrangement of the six oxygen atoms within the same plane. Apart from the chelating nature of one of the DMADB ligands, the structure of **8** is similar to those of $\text{Ba}(\text{BH}_4)_2(\text{diglyme})_2$ and $\text{Ba}(\text{BH}_4)_2(18\text{-crown-6})$.⁵⁷ In both of these complexes, the six oxygen atoms from the two diglyme molecules and the 18-crown-6 ligand describe a hexagonal bipyramid, in which the two $\kappa^3\text{H-BH}_4$ groups occupy the axial positions.

The 15-crown-5 adduct **9** is similar to the diglyme compound **8** in that two molecules of this Lewis base are coordinated per barium atom. The barium atom is sandwiched between the two 15-crown-5 ligands, with the 10 oxygen atoms describing a pentagonal antiprism (Figure 7). Correspondingly, the DMADB groups are counterions and do not coordinate directly to the barium center; they are the first structurally characterized example of $[\text{H}_3\text{BNMe}_2\text{BH}_3]^-$ anions free of any metal interactions. The antiprism sandwich structure of the cation in **9** is identical with that previously reported for the perchlorate salt $[\text{Ba}(15\text{-crown-5})_2][\text{ClO}_4]_2 \cdot 2\text{H}_2\text{O}$.⁷⁰

Finally, compound **10** is an unusual complex salt in which the crown ether groups bind exclusively to the sodium counterions (Figure 8). If each BH_3 unit is considered to occupy one coordination site, then the coordination geometry about the barium anion can best be thought of as a distorted trigonal dodecahedron in which B(1), B(2), B(3), and B(4) make up one of the trapezoids and B(5), B(6), O(1), and O(2) make up the other. All three of the aminodiboranate ligands are bound to barium in a $\kappa^2\text{H-H}_3\text{BNMe}_2\text{BH}_3\text{-}\kappa^2\text{H}$ fashion. The THF ligands are approximately trans with respect to one other with a O(1)–Ba(1)–O(2) bond angle of 166.31(9)°. Despite the relatively high coordination number of 14 (12 hydrogen atoms and 2 oxygen atoms), the Ba...B bond distances are similar to those observed for the other complexes, probably because more of the 14 coordinating atoms are hydrogen.

NMR Spectra. The Ba(DMADB) complexes are insoluble in noncoordinating solvents such as benzene and toluene but are soluble in THF and/or dimethyl sulfoxide (DMSO), which were used to obtain the NMR data (Table 3). In THF- d_8 , the ^1H NMR spectra of **1'**, **2**, **5'**–**8**, and **10** are very similar. All reveal a singlet for the NMe_2 group of the DMADB ligand between δ 2.21 and 2.25 and a broad 1:1:1:1 quartet ($J_{\text{BH}} \sim 90$ Hz) between δ 1.66 and 1.81 for the BH_3 groups. The ^{11}B NMR spectra for **1'**, **2**, **5'**–**8**, and **10** all contain a binomial

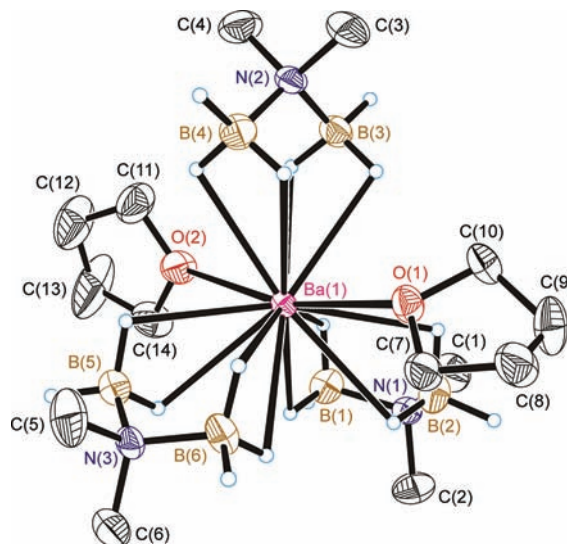


Figure 8. Molecular structure of the $[\text{Ba}(\text{H}_3\text{BNMe}_2\text{BH}_3)_3(\text{THF})_2]^-$ anion in **10**. Ellipsoids are drawn at the 35% probability level. The $[\text{Na}(12\text{-crown-4})_2]^+$ cation and the hydrogen atoms attached to carbon atoms have been omitted for clarity.

Table 3. Selected NMR Chemical Shifts for Barium (*N,N*-Dimethylamino)diboranates^a

cmpd	Lewis base	solvent	^1H (NMe_2)	^1H (BH_3)	^{11}B
1'	Et_2O	$\text{THF-}d_8$	2.23	1.81 (87)	−7.6 (91)
2	DME	$\text{THF-}d_8$	2.23	1.80 (87)	−7.6 (91)
3	TMEDA	$\text{DMSO-}d_6$	2.09	1.39 (91)	−8.6 (92)
4	12-crown-4	$\text{DMSO-}d_6$	2.10	1.39 (91)	−8.6 (92)
5	18-crown-6	$\text{THF-}d_8$	2.23	1.66 (91)	−8.2 (91) ^b
6	teed	$\text{THF-}d_8$	2.24	1.80 (89)	−7.8 (89)
7	PMDTA	$\text{THF-}d_8$	2.25	1.78 (91)	−7.9 (91)
8	diglyme	$\text{THF-}d_8$	2.23	1.79 (87)	−7.6 (91)
9	15-crown-5	$\text{DMSO-}d_6$	2.09	1.25 (92)	−8.8 (92)
10	THF	$\text{THF-}d_8$	2.21	1.66 (91)	−8.7 (91)

^aThe values in parentheses are measured J_{BH} coupling constants in Hz.

^bCollected in $\text{DMSO-}d_6$.

quartet ($J_{\text{BH}} \sim 90$ Hz) between δ −7.6 and −8.7; these resonances are shifted slightly to lower field relative to $\text{Na}(\text{H}_3\text{BNMe}_2\text{BH}_3)$ (δ −10.1). A similar trend is observed upon comparison of the chemical shifts of $\text{Ba}(\text{BH}_4)_2(\text{THF})_2$ (δ −31.4) and NaBH_4 (δ −42.2) in THF.^{57,62} In $\text{DMSO-}d_6$, the ^1H NMR spectra of the TMEDA, 12-crown-4, and 15-crown-5 complexes **3**, **4**, and **9**, respectively, are similar to those described

above: the spectra contain a singlet near δ 2.09 for the NMe_2 resonance of the DMADB ligand and a 1:1:1:1 quartet at either δ 1.39 (3 and 4) or δ 1.25 (9) for the BH_3 groups. The ^{11}B NMR shifts are δ -8.6 for 3 and 4 and δ -8.8 for 9. The three hydrogen atoms on each BH_3 group are chemically equivalent at this temperature because of rapid exchange on the NMR time scale, as is typically observed for borohydride complexes.⁷¹ The ^1H NMR resonances due to the Lewis bases closely match the reported values for the free ligands, which may indicate that they are displaced from the metal in solution by these donor solvents.^{72,73}

If the structures of these barium complexes are similar to those observed in the solid state (see above), then several different environments for the BH_3 and NR_2 groups should be seen in the ^1H NMR spectra; similarly, several of the functional groups in the donor ligands should be diastereotopic. In contrast, the ^1H NMR spectra show only one environment for each of these functional groups. We conclude that the complexes must be dynamic on the NMR time scale in solution. We made no attempt to record spectra below room temperature.

IR and Mass Spectra. Typically, the IR spectra of DMADB complexes exhibit two groups of B–H stretching bands, one for terminal B–H groups at higher frequency and the other for bridging B–H groups at lower frequency. For example, the terminal B–H and bridging B–H–M stretching frequencies in $\text{Mg}(\text{H}_3\text{BNMe}_2\text{BH}_3)_2$ are 2449 and 2195 cm^{-1} , respectively, a separation of 254 cm^{-1} .⁶⁴ Similarly, large frequency differences between the terminal and bridging bands are observed in the spectra of many transition-metal,⁷⁴ lanthanide,⁶⁶ and actinide DMADB complexes,^{75,76} most of which exhibit properties of “covalent” borohydride complexes: high volatility and solubility in nonpolar solvents.⁷⁷ In contrast, ionic DMADB complexes exhibit only small separations between the two sets of B–H stretches: in $\text{Na}(\text{H}_3\text{BNMe}_2\text{BH}_3)$, for example, the separation is only 68 cm^{-1} .⁶² These two peaks have been assigned to the symmetric and asymmetric stretching modes of the BH_3 group rather than to terminal and bridging B–H stretches.⁶² The IR spectra of 1–10 closely resemble that of $\text{Na}(\text{H}_3\text{BNMe}_2\text{BH}_3)$. In all cases, the two sets of B–H stretching bands are separated by less than 101 cm^{-1} and generally are 50–80 cm^{-1} . This finding suggests that the M–H–B bonding is relatively weak and ionic in all of the barium complexes.

Field-desorption mass spectra (FD-MS) of the TMEDA compound 3 and the diglyme compound 8 at high emitter currents show a peak envelope at m/z 491 corresponding to $\text{Ba}_2(\text{H}_3\text{BNMe}_2\text{BH}_3)_3^+$. A peak at m/z 210 corresponding to $\text{Ba}(\text{H}_3\text{BNMe}_2\text{BH}_3)^+$ was also observed in the spectrum of 8. No barium-containing ions were seen in the FD-MS or field-ionization mass spectra of any of the other complexes.

Melting Points and Volatility Studies. The diglyme adduct 8 melts sharply at 102 °C, whereas compounds 1–7, 9, and 10 do not melt even at temperatures as high as 215 °C. Most of the compounds exhibit signs of decomposition during these studies. For example, heating 1' and 2 results in the deposition of colorless crystals on the cooler parts of the melting point capillaries. The crystals almost certainly consist of the aminoborane (H_2BNMe_2), which as we have shown in other studies is the principal thermolysis product of metal complexes containing the DMADB ligand.⁷⁶ Despite the high volatility of magnesium, transition-metal, and lanthanide (dimethylamino)-diboranate compounds, none of the barium complexes is appreciably volatile up to 200 °C at 10^{-2} Torr.^{64,66,74}

DISCUSSION

To be useful for CVD of conformal thin films on advanced architectures, metal-containing precursors should be highly volatile.¹² To achieve this goal, the ligands must be sufficiently large to saturate (or nearly saturate) the coordination sphere of the metal atom, and to prevent the formation of nonvolatile polymers. In addition, the ligands must be thermally robust and sufficiently strongly bound to the metal so that the complexes sublime rather than decompose when heated. However, the ligands must also be bound weakly enough that they dissociate in the deposition zone. The present results show that, even though the (*N,N*-dimethylamino)diboranate ligand satisfies all of these criteria for many metals in the periodic table, it does not do so for barium.

The first shortcoming is that the DMADB ligand is not large enough to saturate the coordination sphere of the Ba^{2+} ion. Even when the barium (DMADB) complexes are provided with Et_2O , DME, and TMEDA ligands as ancillary Lewis bases, the resulting heteroleptic complexes are still polymeric. We have, however, been able to obtain a dimeric complex with the somewhat more sterically demanding ligand TEEDA and monomeric complexes with the assistance of multidentate Lewis bases such as 12-crown-4, 18-crown-6, diglyme, and PMDTA. Interestingly, in the diglyme complex 8, the steric demands of the chelating ether ligands force one of the DMADB ligands to bind to barium through only one of its BH_3 groups rather than to both. This result demonstrates that care must be taken in the choice of an ancillary Lewis base. If the Lewis base is too strongly coordinating or too sterically demanding, it can displace coordinated BH_3 groups or yield salts with charge-separated DMADB anions. An extreme example of this phenomenon is observed in the structure of the 15-crown-5 complex 9, in which the barium center is ligated exclusively by two crown ether molecules, $[\text{Ba}(15\text{-crown-5})_2]^{2+}$, and the $[\text{H}_3\text{BNMe}_2\text{BH}_3]^-$ groups are charge-separated counterions.

The second shortcoming of the DMADB group is that the Ba–H–B bonding in barium (DMADB) complexes is weak and probably highly ionic. This conclusion is drawn from the properties of the barium complexes, which are more similar to those of $\text{Na}(\text{H}_3\text{BNMe}_2\text{BH}_3)$ than to those of the group 2 congener $\text{Mg}(\text{H}_3\text{BNMe}_2\text{BH}_3)_2$. For comparison, $\text{Mg}(\text{H}_3\text{BNMe}_2\text{BH}_3)_2$ is highly soluble in nonpolar solvents (benzene and toluene), has a low melting point, and is highly volatile, whereas the barium complexes and $\text{Na}(\text{H}_3\text{BNMe}_2\text{BH}_3)$ possess none of these properties. Furthermore, the weakness of the metal–ligand bonding in barium (DMADB) complexes is evident in the small frequency separation between the terminal and bridging B–H stretches in the IR spectra, which are similar to those seen for the sodium salt and much smaller than those observed in the magnesium analogue.

Despite the fact that these barium (DMADB) complexes are not particularly volatile, the reaction chemistry of the DMADB ligand remains well poised for the deposition of barium oxide films, as was previously established with lanthanide and magnesium DMADB complexes.^{65,66,74} CVD techniques such as aerosol-assisted CVD (AA-CVD) have been designed to overcome the limitations of precursors with low volatility so that favorable reaction chemistry can be exploited in CVD processes.⁷⁸ Although techniques such as AA-CVD are not well suited for depositing conformal films on substrates with advanced architectures, they may be useful for depositing barium-containing films from the reported DMADB precursors

on relatively flat substrates. At present, we are exploring this possibility and continuing to search for highly volatile barium precursors that possess useful reaction chemistry to address these long-standing problems in the CVD of barium-containing films.

EXPERIMENTAL SECTION

All operations were carried out in a vacuum or under argon using standard Schlenk techniques. All glassware was dried in an oven at 150 °C, assembled hot, and allowed to cool under vacuum before use. Tetrahydrofuran (THF), 1,2-dimethoxyethane (DME), diethyl ether (Et₂O), and pentane were distilled under nitrogen from sodium/benzophenone and degassed with argon immediately before use. Bis(2-methoxyethyl) ether (diglyme) and *N,N,N',N'*-tetramethylethylenediamine (TMEDA) were purchased from Aldrich and distilled from sodium under argon. The crown ethers 12-crown-4 (Avocado Research), and 15-crown-5 (Aldrich) were dried over Linde 4A sieves (Aldrich). Anhydrous BaBr₂ (Strem), 18-crown-6 (Aldrich), *N,N,N',N'*-tetraethylethylenediamine (TEEDA; Aldrich), and *N,N,N',N''*-pentamethyldiethylenetriamine (PMDTA; Aldrich) were used as received. The salt Na(H₃BNMe₂BH₃) was prepared by a literature route.^{62,79}

Elemental analyses were carried out by the University of Illinois Microanalytical Laboratory. The IR spectra were recorded on a Nicolet Impact 410 IR spectrometer as Nujol mulls between KBr plates. The NMR data were collected on a General Electric GN300WB instrument at 7.00 T (¹B), a Varian Unity 400 instrument at 9.4 T (¹H and ¹¹B), or a Varian Unity-500 spectrometer at 11.75 T (¹H). Chemical shifts are reported in δ units (positive shifts to high frequency) relative to SiMe₄ (¹H) or BF₃·Et₂O (¹¹B). Field-desorption (FD-MS) and field-ionization (FI-MS) mass spectra were recorded on a Micromass 70-VSE mass spectrometer. The shapes of all peak envelopes correspond with those calculated from the natural-abundance isotopic distributions in the observed spectra. Melting points were determined in closed capillaries under argon on a Thomas-Hoover Unimelt apparatus.

Bis[(*N,N*-dimethylamino)diboranato]bis(diethyl ether)barium, Ba(H₃BNMe₂BH₃)₂(Et₂O)₂ (1). To a suspension of BaBr₂ (1.00 g, 3.37 mmol) and Na(H₃BNMe₂BH₃) (0.638 g, 6.73 mmol) in THF (1 mL) was added diethyl ether (30 mL) to give a white slurry. As the reaction proceeded, the mixture became homogeneous. After 17 h, the solvent was removed under vacuum to afford a white residue. The residue was extracted with diethyl ether (3 × 15 mL). The extracts were filtered, and the filtrates were combined, concentrated to ca. 20 mL, and cooled to -20 °C to yield white needles suitable for X-ray diffraction. The crystals readily lose Et₂O to form 1', as described below, and microanalytical data for the solvate could not be obtained.

Desolvation of Bis[(*N,N*-dimethylamino)diboranato]bis(diethyl ether)barium(II), Ba(H₃BNMe₂BH₃)₂ (1'). Crystals of 1 from the procedure above were left under dynamic vacuum at room temperature for 12 h. Yield: 0.33 g (63%). Mp: >215 °C. Anal. Calcd for Ba(H₃BNMe₂BH₃)₂(Et₂O)_{0.45}: C, 22.2; H, 9.14; N, 8.92. Found: C, 22.1; H, 9.28; N, 8.62. ¹H NMR (THF-*d*₆, 20 °C): δ 1.81 (br 1:1:1:1 q, *J*_{BH} = 87 Hz, BH₃, 12 H), 2.23 (s, NMe₂, 12 H). ¹¹B NMR (THF-*d*₆, 20 °C): δ -7.6 (q, *J*_{BH} = 91 Hz, BH₃). IR (cm⁻¹): 2398 sh, 2306 vs, 2246 vs, 2091 w, 1217 s, 1194 sh, 1176 s, 1150 s, 1103 w, 1030 s, 951 m, 910 m, 805 w, 413 w. In a similar experiment on a different sample of 1, the desolvated product had a stoichiometry close to Ba(H₃BNMe₂BH₃)₂(Et₂O)_{0.30}. Anal. Calcd: C, 20.6; H, 8.98; N, 9.24. Found: C, 20.8; H, 9.11; N, 9.32. Heating this same sample at 100 °C at 10⁻² Torr for 24 h yields 1', which contains less than 0.1 equiv of diethyl ether per formula unit. Anal. Calcd: C, 17.6; H, 8.67; N, 9.87. Found: C, 17.6; H, 8.41; N, 9.66.

Bis[(*N,N*-dimethylamino)diboranato](1,2-dimethoxyethane)barium(II), Ba(H₃BNMe₂BH₃)₂(DME) (2). To a solution of 1' (0.073 g, 0.23 mmol) in diethyl ether (10 mL) was added DME (10 mL). The solution was evaporated to dryness under vacuum to yield a white solid. Yield: 0.075 g (88%). Crystals of 2 suitable for diffraction studies can be grown by cooling saturated Et₂O solutions to -20 °C. Mp:

>215 °C. Anal. Calcd for C₈H₃₄B₄N₂O₂Ba: C, 25.9; H, 9.24; N, 7.55. Found: C, 26.3; H, 9.59; N, 7.11. ¹H NMR (THF-*d*₆, 20 °C): δ 1.80 (br 1:1:1:1 q, *J*_{BH} = 87 Hz, BH₃, 12 H), 2.23 (s, NMe₂, 12 H), 3.27 (s, OMe, 6 H), 3.43 (s, OCH₂, 4 H). ¹¹B NMR (THF-*d*₆, 20 °C): δ -7.6 (q, *J*_{BH} = 91 Hz, BH₃). IR (cm⁻¹): 2309 vs, 2287 sh, 2242 s, 1192 m, 1176 s, 1150 s, 1119 w, 1100 w, 1071 s, 1027 s, 948 m, 907 m, 859 m, 837 w, 805 m.

Bis[(*N,N*-dimethylamino)diboranato](*N,N,N',N'*-tetramethylethylenediamine)barium(II), Ba(H₃BNMe₂BH₃)₂(TMEDA) (3). To a solution of 1' (0.16 g, 0.51 mmol) in diethyl ether (30 mL) was added TMEDA (0.25 mL, 1.7 mmol). A thick white precipitate formed immediately. The mixture was stirred overnight, and then the solid was collected by filtration, washed with pentane (3 × 20 mL), and dried under vacuum to yield a white powder. Yield: 0.19 g (94%). Crystals of 3 suitable for diffraction studies can be grown by cooling saturated solutions in Et₂O to -20 °C. Mp: >215 °C. Anal. Calcd for C₁₀H₄₀B₄N₄Ba: C, 30.3; H, 10.2; N, 14.1. Found: C, 30.3; H, 10.8; N, 13.6. ¹H NMR (DMSO-*d*₆, 20 °C): δ 1.39 (1:1:1:1 q, *J*_{BH} = 91 Hz, BH₃, 12 H), 2.09 (br s, DMADB NMe₂, 12 H), 2.11 (s, TMEDA NMe₂, 6 H), 2.27 (s, NCH₂, 4 H). ¹¹B NMR (DMSO-*d*₆, 20 °C): δ -8.6 (q, *J*_{BH} = 92 Hz, BH₃). MS (FD) [fragment ion, relative abundance]: *m/z* 491 [Ba₂(H₃BNMe₂BH₃)₃⁺, 100]. IR (cm⁻¹): 2794 m, 2778 m, 2379 m, 2309 vs, 2283 vs, 2255 s, 2243 vs, 2090 w, 1293 m, 1245 w, 1213 s, 1192 w, 1176 s, 1154 vs, 1128 m, 1078 w, 1027 s, 954 m, 942 m, 919 w, 908 w, 808 m, 786 m, 697 w, 574 w, 438 w, 413 w.

Bis[(*N,N*-dimethylamino)diboranato](12-crown-4)barium(II), Ba(H₃BNMe₂BH₃)₂(12-crown-4) (4). To a solution of 1' (0.10 g, 0.32 mmol) in diethyl ether (25 mL) was added 12-crown-4 (70 μL, 0.43 mmol). A thick white precipitate formed immediately. The mixture was stirred overnight, and then the solid was collected by filtration, washed with pentane (3 × 20 mL), and dried under vacuum to yield a white powder. Yield: 0.14 g (96%). Mp: >215 °C. Anal. Calcd for C₁₂H₄₀B₄N₂O₄Ba: C, 31.5; H, 8.82; N, 6.13. Found: C, 31.6; H, 9.00; N, 5.67. ¹H NMR (DMSO-*d*₆, 20 °C): δ 1.39 (1:1:1:1 q, *J*_{BH} = 91 Hz, BH₃, 12 H), 2.10 (br s, NMe₂, 12 H), 3.56 (s, OCH₂, 16 H). ¹¹B NMR (DMSO-*d*₆, 20 °C): δ -8.6 (q, *J*_{BH} = 92 Hz, BH₃). IR (cm⁻¹): 2394 w, 2340 w, 2303 vs, 2249 s, 1305 w, 1290 w, 1248 w, 1216 m, 1205 m, 1177 s, 1149 s, 1133 m, 1086 s, 1018 vs, 933 w, 921 m, 904 w, 852 s, 800 w, 561 w, 548 w.

Bis[(*N,N*-dimethylamino)diboranato](12-crown-4)-(tetrahydrofuran)barium(II)-tetrahydrofuran, Ba(H₃BNMe₂BH₃)₂(12-crown-4)(THF)·THF (4'). Cooling saturated solutions of 4 in THF to -20 °C produced crystals of the solvate 4' suitable for diffraction studies. The crystals readily desolvated to form 4, and microanalytical data for 4' could not be obtained.

Bis[(*N,N*-dimethylamino)diboranato](18-crown-6)barium(II), Ba(H₃BNMe₂BH₃)₂(18-crown-6) (5). To a solution of 1' (0.13 g, 0.48 mmol) in THF (30 mL) was added 18-crown-6 (0.13 g, 0.48 mmol) to yield a clear colorless solution. After 12 h, the solution was concentrated to ca. 15 mL and cooled to -20 °C to afford colorless platelets. The platelets were collected by filtration, washed with pentane (3 × 5 mL), and evaporated to dryness under vacuum to yield a free-flowing white solid. Yield: 0.047 g (18%). Mp: >215 °C. Anal. Calcd for C₁₆H₄₈B₄N₂O₆Ba: C, 35.2; H, 8.87; N, 5.14. Found: C, 35.0; H, 8.65; N, 5.17. ¹H NMR (THF-*d*₆, 20 °C): δ 1.66 (1:1:1:1 q, *J*_{BH} = 91 Hz, BH₃, 12 H), 2.23 (s, NMe₂, 12 H), 3.78 (s, OCH₂, 24 H). ¹¹B NMR (DMSO-*d*₆, 20 °C): δ -8.2 (q, *J*_{BH} = 91 Hz, BH₃). IR (cm⁻¹): 2366 m, 2285 s, 2233 m, 2182 m, 2084 w, 2065 w, 1378 s, 1349 m, 1286 m, 1246 w, 1200 m, 1175 m, 1149 m, 1088 s, 1046 w, 1013 m, 962 m, 924 m, 904 w, 834 m, 797 w, 723 w.

Bis[(*N,N*-dimethylamino)diboranato](18-crown-6)barium(II)-bis(tetrahydrofuran), Ba(H₃BNMe₂BH₃)₂(18-crown-6)·2THF (5'). Cooling a saturated solution of 5 in THF to -20 °C afforded colorless platelets of the solvate 5' suitable for X-ray diffraction studies. The crystals readily desolvated to form 5, and microanalytical data for 5' could not be obtained.

Bis[(*N,N*-dimethylamino)diboranato](*N,N,N',N'*-tetraethylethylenediamine)barium, Ba(H₃BNMe₂BH₃)₂(TEEDA) (6). To a solution of 1' (0.092 g, 0.30 mmol) in THF (10 mL) was added TEEDA (0.21 mL, 0.98 mmol). After 17 h, the clear colorless solution was

filtered, concentrated to ca. 10 mL, and cooled to $-20\text{ }^{\circ}\text{C}$ to afford large colorless blocks. Yield: 0.071 g (48%). Anal. Calcd for $\text{C}_{14}\text{H}_{48}\text{N}_2\text{B}_4\text{Ba}$: C, 37.1; H, 10.7; N, 12.4. Found: C, 36.9; H, 10.8; N, 12.3. ^1H NMR (THF- d_8): δ 1.12 (t, $J_{\text{HH}} = 7.0$ Hz, β -Et, 12 H), 1.80 (1:1:1:1 q, $J_{\text{BH}} = 89$ Hz, BH_3 , 12 H), 2.24 (s, NMe_2 , 12 H), 2.84 (s, NCH_2CH_2 , 4 H), 3.38 (q, $J_{\text{HH}} = 7.0$ Hz, α -Et, 8 H). ^{11}B NMR (THF- d_8): δ -7.8 (q, $J_{\text{BH}} = 89$ Hz). IR (cm^{-1}): 2423 sh, 2392 w, 2308 vs, 2257 s, 2239 sh, 2119 w, 2103 w, 2082 w, 2064 w, 1374 s, 1349 m, 1314 w, 1245 w, 1211 s, 1174 s, 1147 s, 1101 w, 1088 m, 1052 m, 1029 m, 1013 m, 990 w, 954 m, 926 m, 908 m, 813 m, 795 m, 740 w, 724 w, 563 w, 549 w, 526 w.

Bis[(*N,N*-dimethylamino)diboranato](*N,N,N',N'',N''*-pentamethyldiethylenetriamene)barium, $\text{Ba}(\text{H}_3\text{BNMe}_2\text{BH}_3)_2(\text{PMDTA})(7)$. To a solution of **1'** (0.50, 1.6 mmol) in THF (20 mL) was added *N,N,N',N'',N''*-pentamethyldiethylenetriamine (1.1 mL, 5.4 mmol). After 17 h, the clear colorless solution was filtered, concentrated to ca. 20 mL, and cooled to $-20\text{ }^{\circ}\text{C}$ to afford large colorless prisms. Yield: 0.16 g (20%). Anal. Calcd for $\text{C}_{13}\text{H}_{47}\text{N}_3\text{B}_4\text{Ba}$: C, 34.4; H, 10.4; N, 15.4. Found: C, 34.7; H, 10.8; N, 15.6. ^1H NMR (THF- d_8): δ 1.78 (1:1:1:1 q, $J_{\text{BH}} = 91$ Hz, BH_3 , 12 H), 2.18 (s, NMe_2 , 12 H), 2.24 (s, NMe , 3 H), 2.25 (s, NMe_2 , 12 H), 2.39 (m, NCH_2 , 8 H). ^{11}B NMR (THF- d_8): δ -7.9 (q, $J_{\text{BH}} = 91$ Hz). IR (cm^{-1}): 2393 m, 2300 s, 2272 s, 2246 s, 1352 w, 1310 w, 1297 w, 1246 m, 1216 s, 1176 s, 1148 m, 1104 m, 1104 w, 1081 w, 1016 s, 967 w, 930 m, 901 w, 789 w, 773 w.

Bis[(*N,N*-dimethylamino)diboranato]bis[bis(2-methoxyethyl) ether]barium(II), $\text{Ba}(\text{H}_3\text{BNMe}_2\text{BH}_3)_2(\text{diglyme})_2(8)$. To BaBr_2 (0.50 g, 1.7 mmol) and $\text{Na}(\text{H}_3\text{BNMe}_2\text{BH}_3)$ (0.32 g, 3.4 mmol) was added bis(2-methoxyethyl) ether (50 mL). After the cloudy mixture had been stirred for 20 h, the solvent was removed by distillation under vacuum to afford a white residue. The residue was extracted with diethyl ether (2×30 mL), the extracts were filtered, and the filtrates were combined, concentrated to ca. 55 mL, and cooled to $-20\text{ }^{\circ}\text{C}$ to yield 0.21 g of white crystals. The mother liquor was concentrated to 10 mL and cooled to $-20\text{ }^{\circ}\text{C}$ to yield an additional 0.10 g of white needles. Yield: 0.31 g (34%). Mp: $102\text{ }^{\circ}\text{C}$. Anal. Calcd for $\text{C}_{16}\text{H}_{32}\text{B}_4\text{N}_2\text{O}_6\text{Ba}$: C, 35.0; H, 9.54; N, 5.10. Found: C, 34.7; H, 9.89; N, 5.06. ^1H NMR (THF- d_8 , $20\text{ }^{\circ}\text{C}$): δ 1.79 (br 1:1:1:1 q, $J_{\text{BH}} = 87$ Hz, BH_3 , 12 H), 2.23 (s, NMe_2 , 12 H), 3.29 (s, OMe , 12 H), 3.46 (m, OCH_2 , 8 H), 3.55 (m, OCH_2 , 8 H). ^{11}B NMR (THF- d_8 , $20\text{ }^{\circ}\text{C}$): δ -7.6 (q, $J_{\text{BH}} = 91$ Hz, BH_3). MS (FD) [fragment ion, relative abundance]: m/z 210 [$\text{Ba}(\text{H}_3\text{BNMe}_2\text{BH}_3)^+$, 100], 491 [$\text{Ba}_2(\text{H}_3\text{BNMe}_2\text{BH}_3)_3^+$, 70]. IR (cm^{-1}): 2340 sh, 2290 vs, 2236 s, 2186 sh, 2069 m, 1353 m, 1302 w, 1258 m, 1203 s, 1174 s, 1150 vs, 1135 s, 1102 s, 1083 s, 1071 s, 1061 s, 1015 s, 995 m, 942 sh, 925 m, 904 w, 873 sh, 863 s, 830 w, 799 m, 685 w, 529 w, 457 w, 413 w.

Bis[(*N,N*-dimethylamino)diboranato]bis(15-crown-5)barium(II), $[\text{Ba}(15\text{-crown-5})_2][\text{H}_3\text{BNMe}_2\text{BH}_3]_2(9)$. To a solution of **1'** (0.30 g, 1.1 mmol) in THF (30 mL) was added 15-crown-5 (0.28 mL, 1.4 mmol). A white precipitate formed immediately. After 2 h, the solid was collected by filtration and washed with cold THF (5 mL) and pentane (2×10 mL) to yield a flocculent white powder. Extracting the solid with hot THF (ca. 20 mL) at $60\text{ }^{\circ}\text{C}$ followed by slow cooling of the filtrate to room temperature afforded colorless platelets. Yield: 0.25 g (94%). Mp: $>215\text{ }^{\circ}\text{C}$. Anal. Calcd for $\text{C}_{24}\text{H}_{64}\text{B}_4\text{N}_2\text{O}_5\text{Ba}$: C, 40.0; H, 8.94; N, 3.88. Found: C, 39.6; H, 8.86; N, 3.83. ^1H NMR (DMSO- d_6 , $20\text{ }^{\circ}\text{C}$): δ 1.25 (1:1:1:1 q, $J_{\text{BH}} = 92$ Hz, BH_3 , 12 H), 2.09 (br s, NMe_2 , 12 H), 3.54 (s, OCH_2 , 40 H). ^{11}B NMR (DMSO- d_6 , $20\text{ }^{\circ}\text{C}$): δ -8.8 (q, $J_{\text{BH}} = 92$ Hz, BH_3). IR (cm^{-1}): 2338 m, 2297 s, 2266 s, 2197 m, 2168 sh, 2050 w, 1375 s, 1301 m, 1255 m, 1179 s, 1155 m, 1116 s, 1078 m, 1008 m, 946 m, 914 m, 857 m, 722 m.

Bis(12-crown-4)sodium Tris[(*N,N*-dimethylamino)diboranato]bis(tetrahydrofuran)borate, $[\text{Na}(12\text{-crown-4})_2][\text{Ba}(\text{H}_3\text{BNMe}_2\text{BH}_3)_3(\text{THF})_2](10)$. To a suspension of BaBr_2 (0.17 g, 0.61 mmol) and $\text{Na}(\text{H}_3\text{BNMe}_2\text{BH}_3)$ (0.12 g, 1.2 mmol) in THF (1 mL) was added diethyl ether (30 mL). After 17 h, the white slurry was filtered and the filtrate was taken to dryness in a vacuum. The white solid was dissolved in THF (25 mL) and treated with 12-crown-4 (0.099 mL, 0.61 mmol) to afford a clear colorless solution, which turned cloudy after about 20 min. The mixture was filtered, and the filtrate was concentrated to ca. 15 mL and cooled to $-20\text{ }^{\circ}\text{C}$ to afford

colorless prisms. Yield: 0.18 g (41%). Anal. Calcd for $\text{C}_{30}\text{H}_{84}\text{N}_3\text{O}_{10}\text{NaBa}$: C, 41.3; H, 9.71; N, 4.82. Found: C, 41.3; H, 9.87; N, 4.78. ^1H NMR (THF- d_8): δ 1.66 (1:1:1:1 q, $J_{\text{BH}} = 91$ Hz, BH_3 , 18 H), 1.76 (m, β -THF, 8 H), 2.21 (s, NMe_2 , 18 H), 3.60 (m, α -THF, 8 H), 3.65 (s, 12-crown-4, 32 H). ^{11}B NMR (THF- d_8): δ -8.7 (q, $J_{\text{BH}} = 91$ Hz). IR (cm^{-1}): 2391 m, 2351 w, 2291 vs, 2249 s, 2177 m, 1365 m, 1305 m, 1290 m, 1256 m, 1177 s, 1150 s, 1137 s, 1097 s, 1048 s, 1022 s, 919 s, 887 w, 850 m, 795 w, 554 m.

■ ASSOCIATED CONTENT

Supporting Information

Crystallographic details, tables of bond distances and angles, CIF files for compounds **1–3**, **4'**, **5'**, and **6–10**, and diagrams of the molecular structures of **1–3**. This material is available free of charge via the Internet at <http://pubs.acs.org>.

■ AUTHOR INFORMATION

Corresponding Author

*E-mail: gggirolam@illinois.edu.

■ ACKNOWLEDGMENTS

We thank the National Science Foundation (CHE-1112360) and the PG Research Foundation for support of this research, and Scott Wilson, Teresa Wieckowska-Prussak, and Danielle L. Gray for collecting the X-ray diffraction data.

■ REFERENCES

- Phule, P. P.; Risbud, S. H. *J. Mater. Sci.* **1990**, *25*, 1169–1183.
- Wessels, B. W. *Annu. Rev. Mater. Sci.* **1995**, *25*, 525–546.
- Hwang, C. S. *Mater. Sci. Eng., B* **1998**, *B56*, 178–190.
- Vijatovic, M. M.; Bobic, J. D.; Stojanovic, B. D. *Sci. Sintering* **2008**, *40*, 155–165.
- Wu, M. K.; Ashburn, J. R.; Torng, C. J.; Hor, P. H.; Meng, R. L.; Gao, L.; Huang, Z. J.; Wang, Y. Q.; Chu, C. W. *Phys. Rev. Lett.* **1987**, *58*, 908–910.
- Dou, S. X.; Nikheenko, P. N.; Wang, X. L.; Liu, H. K. *Annu. Rep. Prog. Chem., Sect. C* **1997**, *93*, 363–399.
- Fisk, Z.; Sarrao, J. L. *Annu. Rev. Mater. Sci.* **1997**, *27*, 35–67.
- Tretyakov, Y. D.; Goodilin, E. A. *Russ. Chem. Rev.* **2000**, *69*, 1–34.
- Kuppasami, P.; Raghunathan, V. S. *Int. Mater. Rev.* **2003**, *48*, 1–43.
- Lu, J.; Wu, X.; Chen, C.; Liang, J.; Cheng, W. *Chin. Sci. Bull.* **1997**, *42*, 1233–1240.
- Fedorov, P. P.; Kokh, A. E.; Kononova, N. G. *Russ. Chem. Rev.* **2002**, *71*, 651–671.
- Yanguas-Gil, A.; Yang, Y.; Kumar, N.; Abelson, J. R. *J. Vac. Sci. Technol., A* **2009**, *27*, 1235–1243.
- George, S. M. *Chem. Rev.* **2010**, *110*, 111–131.
- Wojtczak, W. A.; Fleig, P. F.; Hampden-Smith, M. J. *Adv. Organomet. Chem.* **1996**, *40*, 215–340.
- Matthews, J. S.; Rees, W. S. Jr. *Adv. Inorg. Chem.* **2000**, *50*, 173–192.
- Vehkamäki, M.; Hatanpää, T.; Hänninen, T.; Ritala, M.; Leskelä, M. *Electrochem. Solid-State Lett.* **1999**, *2*, 504–506.
- Harvey, M. J.; Quisenberry, K. T.; Hanusa, T. P.; Young, V. G. *Eur. J. Inorg. Chem.* **2003**, 3383–3390.
- El-Kaderi, H. M.; Heeg, M. J.; Winter, C. H. *Polyhedron* **2006**, *25*, 224–234.
- Harvey, M. J.; Burkey, D. J.; Chmely, S. C.; Hanusa, T. P. *J. Alloys Compd.* **2009**, *488*, 528–532.
- Saly, M. J.; Heeg, M. J.; Winter, C. H. *Polyhedron* **2011**, *30*, 1330–1338.
- Saly, M. J.; Winter, C. H. *Organometallics* **2011**, *29*, 5472–5480.
- Sedai, B.; Heeg, M. J.; Winter, C. H. *Organometallics* **2009**, *28*, 1032–1038.

- (23) Condorelli, G. G.; Malandrino, G.; Fragalà, I. L. *Coord. Chem. Rev.* **2007**, *251*, 1931–1950.
- (24) Tammenmaa, M.; Antson, H.; Asplund, M.; Hiltunen, L.; Leskelä, M.; Niinistö, L.; Ristolainen, E. *J. Cryst. Growth* **1987**, *84*, 151–154.
- (25) Purdy, A. P.; Berry, A. D.; Holm, R. T.; Fatemi, M.; Gaskill, D. K. *Inorg. Chem.* **1989**, *28*, 2799–2803.
- (26) Gardiner, R.; Brown, D. W.; Kirilin, P. S.; Rheingold, A. L. *Chem. Mater.* **1991**, *3*, 1053–1059.
- (27) Wills, L. A.; Wessels, B. W.; Richeson, D. S.; Marks, T. J. *Appl. Phys. Lett.* **1992**, *60*, 41–43.
- (28) Sievers, R. E.; Turnipseed, S. B.; Huang, L.; Lagalante, A. F. *Coord. Chem. Rev.* **1993**, *128*, 285–291.
- (29) Belot, J. A.; Neumayer, D. A.; Reedy, C. J.; Studebaker, D. B.; Hinds, B. J.; Stern, C. L.; Marks, T. J. *Chem. Mater.* **1997**, *9*, 1638–1648.
- (30) Tiitta, M.; Niinistö, L. *Chem. Vap. Deposition* **1997**, *3*, 167–182.
- (31) Saanila, V.; Ihanus, J.; Ritala, M.; Leskelä, M. *Chem. Vap. Deposition* **1998**, *4*, 227–233.
- (32) Dhote, A. M.; Meier, A. L.; Towner, D. J.; Wessels, B. W.; Ni, J.; Marks, T. J. *J. Vac. Sci. Technol., B* **2005**, *23*, 1674–1678.
- (33) Nilsen, O.; Rauwel, E.; Fjellvag, H.; Kjekshus, A. J. *Mater. Chem.* **2007**, *17*, 1466–1475.
- (34) Wersand-Quell, S.; Orsal, G.; Thevenin, P.; Bath, A. *Thin Solid Films* **2007**, *515*, 6507–6511.
- (35) Schulz, D. L.; Hinds, B. J.; Neumayer, D. A.; Stern, C. L.; Marks, T. J. *Chem. Mater.* **1993**, *5*, 1605–1617.
- (36) Neumayer, D. A.; Belot, J. A.; Feezel, R. L.; Reedy, C.; Stern, C. L.; Marks, T. J.; Liable-Sands, L. M.; Rheingold, A. L. *Inorg. Chem.* **1998**, *37*, 5625–5633.
- (37) Studebaker, D. B.; Neumayer, D. A.; Hinds, B. J.; Stern, C. L.; Marks, T. J. *Inorg. Chem.* **2000**, *39*, 3148–3157.
- (38) Aspinall, H. C. *Top. Appl. Phys.* **2007**, *106*, 53–72.
- (39) Chi, Y.; Ranjan, S.; Chou, T.-Y.; Liu, C.-S.; Peng, S.-M.; Lee, G.-H. *J. Chem. Soc., Dalton Trans.* **2001**, 2462–2466.
- (40) Ihanus, J.; Hänninen, T.; Hatanpää, T.; Aaltonen, T.; Mutikainen, I.; Sajavaara, T.; Keinonen, J.; Ritala, M.; Leskelä, M. *Chem. Mater.* **2002**, *14*, 1937–1944.
- (41) Hatanpää, T.; Vehkamäki, M.; Mutikainen, I.; Kansikas, J.; Ritala, M.; Leskelä, M. *Dalton Trans.* **2004**, 1181–1188.
- (42) Ihanus, J.; Hänninen, T.; Hatanpää, T.; Ritala, M.; Leskelä, M. *J. Electrochem. Soc.* **2004**, *151*, H221–H225.
- (43) Putkonen, M.; Niinistö, L. *Top. Organomet. Chem.* **2005**, *9*, 125–145.
- (44) Hatanpää, T.; Ritala, M.; Leskelä, M. *J. Organomet. Chem.* **2007**, *692*, 5256–5262.
- (45) Vehkamäki, M.; Hatanpää, T.; Ritala, M.; Leskelä, M.; Vayrynen, S.; Rauhala, E. *Chem. Vap. Deposition* **2007**, *13*, 239–246.
- (46) Malandrino, G.; Lo Nigro, R.; Fragalà, I. L. *Chem. Vap. Deposition* **2007**, *13*, 651–655.
- (47) Saly, M. J.; Heeg, M. J.; Winter, C. H. *Inorg. Chem.* **2009**, *48*, 5303–5312.
- (48) Saly, M. J.; Munnik, F.; Baird, R. J.; Winter, C. H. *Chem. Mater.* **2009**, *21*, 3742–3744.
- (49) Jensen, J. A.; Gozum, J. E.; Pollina, D. M.; Girolami, G. S. *J. Am. Chem. Soc.* **1988**, *110*, 1643–1644.
- (50) Sung, J.; Goedde, D. M.; Girolami, G. S.; Abelson, J. R. *J. Appl. Phys.* **2002**, *91*, 3904–3911.
- (51) Jayaraman, S.; Yang, Y.; Kim, D. Y.; Girolami, G. S.; Abelson, J. R. *J. Vac. Sci. Technol., A* **2005**, *23*, 1619–1625.
- (52) Yang, Y.; Jayaraman, S.; Kim, D. Y.; Girolami, G. S.; Abelson, J. R. *J. Cryst. Growth* **2006**, *294*, 389–395.
- (53) Yang, Y.; Jayaraman, S.; Kim, D. Y.; Girolami, G. S.; Abelson, J. R. *Chem. Mater.* **2006**, *18*, 5088–5096.
- (54) Kumar, N.; Yang, Y.; Noh, W.; Girolami, G. S.; Abelson, J. R. *Chem. Mater.* **2007**, *19*, 3802–3807.
- (55) Yang, Y.; Jayaraman, S.; Sperling, B.; Kim, D. Y.; Girolami, G. S.; Abelson, J. R. *J. Vac. Sci. Technol., A* **2007**, *25*, 200–206.
- (56) Kumar, N.; Yanguas-Gil, A.; Daly, S. R.; Girolami, G. S.; Abelson, J. R. *J. Am. Chem. Soc.* **2008**, *130*, 17660–17661.
- (57) Bremer, M.; Nöth, H.; Thomann, M.; Schmidt, M. *Chem. Ber.* **1995**, *128*, 455–460.
- (58) Cerny, R.; Filinchuk, Y.; Hagemann, H.; Yvon, K. *Angew. Chem., Int. Ed.* **2007**, *46*, 5765–5767.
- (59) Goedde, D. M.; Windler, G. K.; Girolami, G. S. *Inorg. Chem.* **2007**, *46*, 2814–2823.
- (60) Keller, P. C. *J. Chem. Soc. D* **1969**, 1465.
- (61) Keller, P. C. *Inorg. Chem.* **1971**, *10*, 2256–2259.
- (62) Nöth, H.; Thomas, S. *Eur. J. Inorg. Chem.* **1999**, 1373–1379.
- (63) Kim, D. Y.; Yang, Y.; Abelson, J. R.; Girolami, G. S. *Inorg. Chem.* **2007**, *46*, 9060–9066.
- (64) Kim, D. Y.; Girolami, G. S. *Inorg. Chem.* **2010**, *49*, 4942–4948.
- (65) Kumar, N.; Yanguas-Gil, A.; Daly, S. R.; Girolami, G. S.; Abelson, J. R. *Appl. Phys. Lett.* **2009**, *95*, 144107/144101–144107/144103.
- (66) Daly, S. R.; Kim, D. Y.; Yang, Y.; Abelson, J. R.; Girolami, G. S. *J. Am. Chem. Soc.* **2010**, *132*, 2106–2107.
- (67) Izod, K.; Wills, C.; Clegg, W.; Harrington, R. W. *Inorg. Chem.* **2007**, *46*, 4320–4325.
- (68) Bondi, A. J. *Phys. Chem.* **1964**, *68*, 441–451.
- (69) Ruiz-Martinez, A.; Casanova, D.; Alvarez, S. *Chem.–Eur. J.* **2008**, *14*, 1291–1303.
- (70) Junk, P. C.; Steed, J. W. *J. Coord. Chem.* **2007**, *60*, 1017–1028.
- (71) Eaton, G. R.; Lipscomb, W. N. *NMR Studies of Boron Hydrides and Related Compounds*; Benjamin: New York, 1969.
- (72) Gottlieb, H. E.; Kotlyar, V.; Nudelman, A. *J. Org. Chem.* **1997**, *62*, 7512–7515.
- (73) Fulmer, G. R.; Miller, A. J. M.; Sherden, N. H.; Gottlieb, H. E.; Nudelman, A.; Stoltz, B. M.; Bercaw, J. E.; Goldberg, K. I. *Organometallics* **2010**, *29*, 2176–2179.
- (74) Girolami, G. S.; Kim, D. Y.; Abelson, J. R.; Kumar, N.; Yang, Y.; Daly, S. U.S. Pat. Appl. 59728, April 9, 2008.
- (75) Daly, S. R.; Girolami, G. S. *Inorg. Chem.* **2010**, *49*, 5157–5166.
- (76) Daly, S. R.; Piccoli, P. M. B.; Schultz, A. J.; Todorova, T. K.; Gagliardi, L.; Girolami, G. S. *Angew. Chem., Int. Ed.* **2010**, *49*, 3379–3381.
- (77) Marks, T. J.; Kolb, J. R. *Chem. Rev.* **1977**, *77*, 263–293.
- (78) Hou, X.; Choy, K.-L. *Chem. Vap. Deposition* **2006**, *12*, 583–596.
- (79) Daly, S. R.; Bellott, B. J.; Kim, D. Y.; Girolami, G. S. *J. Am. Chem. Soc.* **2010**, *132*, 7254–7255.